

Constraints for Use of Ultraviolet Spectropolarimetry to Detect Chiral Amino Acids from Comets

Ana I. Gómez de Castro and Ana I. De Isidro-Gómez

Abstract

Life is pervasive on planet Earth, but whether life is ubiquitous in the Galaxy and sustainable over timescales comparable to stellar evolution is unknown. Evidence suggests that life first appeared on Earth more than 3.77 Gyr ago, during a period of heavy meteoric bombardment. Amino acids, the building blocks of proteins, have been demonstrated to exist in interstellar ice. As such, the contribution of space-generated amino acids to those existing on Earth should be considered. However, detection of space amino acids is challenging. In this study, we used analytical data from several meteorites and *in situ* measurements of the comet 67P/Churyumov-Gerasimenko collected by the Rosetta probe to evaluate the detectability of alanine by ultraviolet spectropolarimetry. Alanine is the second-most abundant amino acid after glycine and is optically active. This chirality produces a unique signature that enables reliable identification of this amino acid using the imprint of optical rotatory dispersion (ORD) and circular dichroism (CD) in the ultraviolet spectrum (130–230 nm). Here, we show that the ORD signature could be detected in comets by using ultraviolet spectropolarimetric observations conducted at middle size space observatories. These observations can also provide crucial information for the study of sources of enantiomeric imbalance on Earth. **Key Words:** Astrobiology—Chirality—Comets—Remote sensing—Ultraviolet spectroscopy. *Astrobiology* 21, 718–728.

1. Introduction

AMINO ACIDS are the building blocks of life. However, the source of amino acids is unclear, particularly with regard to whether they formed on Earth (Miller, 1953; Parker *et al.*, 2011) or were brought by comets (Bernstein *et al.*, 2002; Muñoz Caro *et al.*, 2002; Chen *et al.*, 2008). Both routes have obvious differences and important implications for how amino acids might be dispersed across the Universe (Wickramasinghe, 1974; Martins *et al.*, 2008).

Experiments to reproduce the formation of amino acids on Earth date back to those performed by Miller in 1953. A reducing atmosphere similar to that present soon after the formation of Earth was reproduced in a laboratory setting and used to generate a mixture of amino acids after exposure to electrical discharges (Miller, 1953; Miller and Urey, 1959; Oró, 1967; Cleaves *et al.*, 2008; Parker *et al.*, 2011).

In the early 2000s a new branch of laboratory exploration was initiated by ultraviolet (UV) irradiation of dirty ice to simulate conditions present in comets. In these experiments, photoionization by UV radiation is used to accelerate chemical reactions that form glycine, alanine, and other amino acids (Muñoz Caro *et al.*, 2002). Several experimental ap-

proaches have been used to synthesize proteinogenic amino acids (Table 1), although none of these techniques could produce the full set of amino acids present in proteins. An intriguing question is whether the current amino acid fingerprint on Earth can provide clues about the dominant process by which amino acids originally formed.

A fundamental problem in astrobiology is whether a universal set of amino acids is being formed or if there are significant spatial and temporal deviations across the Universe (Loeb *et al.*, 2016). Such differences could be related to compatibility, at a molecular level, between life-forms. For instance, UV radiation that photoprocesses ices in space is not homogeneous, either now or soon after the Universe was formed. Ice in comets orbiting solar-like stars is exposed to strong radiation at several specific wavelengths (*e.g.*, 121, 155, and 280 nm) (see, *e.g.*, Ayres *et al.* [1995] for main-sequence cool stars or Gómez de Castro and Marcos-Arenal [2012] for pre-main-sequence cool stars), whereas ice in the interstellar medium is subject to the smooth spectral energy distribution of the UV background (see, *e.g.*, Draine, 1978).

Investigations concerning generation of life at a cosmic level have been severely hampered by difficulties with the collection of experimental data and remote detection of even

Universidad Complutense de Madrid, Madrid, Spain.

© Ana I. Gómez de Castro and Ana I. De Isidro-Gómez, 2021; Published by Mary Ann Liebert, Inc. This Open Access article is distributed under the terms of the Creative Commons Attribution Noncommercial License (<http://creativecommons.org/licenses/by-nc/4.0/>) which permits any noncommercial use, distribution, and reproduction in any medium, provided the original author(s) and the source are credited.

TABLE 1. PROTEINOGENIC AMINO ACIDS PRODUCED IN “ORIGINS OF LIFE” EXPERIMENTS TO SIMULATE EARLY EARTH CONDITIONS OR SPACE ICE AND COMETS

Proteinogenic amino acid	Early Earth conditions		Space ice and comets
	Miller, 1952	Parker et al., 2011	Muñoz Caro et al., 2002
Glycine	Produced	Produced	Produced
Alanine	Produced	Produced	Produced
Aspartic acid	Produced	Produced	Produced
Serine		Produced	Produced
Valine		Produced	Produced
Glutamic acid		Produced	
Phenylalanine			
Methionine		Produced	
Isoleucine		Produced	
Leucine		Produced	
Cysteine			
Histidine			
Lysine			
Asparagine			
Pyrrolysine			Produced
Proline			
Glutamine			
Arginine			
Threonine			
Selenocysteine			
Tryptophan			
Tyrosine			

simple compounds like amino acids. To date, only glycine has been conclusively detected by using *in situ* measurements carried out by the Rosetta probe (Altwegg *et al.*, 2016). However, remote detection could be possible if the chirality imbalance observed in many biological molecules on Earth were widespread in the Universe. According to laboratory experiments, in space ice α -alanine (hereafter, alanine) is the second-most abundant amino acid after glycine, with an abundance 40% that of glycine (Muñoz Caro *et al.*, 2002). Unlike glycine, alanine is an optically active molecule. Left and right isomers of alanine are produced naturally, and any imbalance in isomer distribution will produce a clear signature in radiation polarization. Other abundant, optically active amino acids are serine, valine, and proline; however, their abundance relative to that of glycine is significantly smaller (7.2%, 1.2%, and 0.06%, respectively) (see Sandford *et al.*, 2020 and references therein). Thus, they are more difficult to detect even though some of them, such as valine or leucine, display a level of optical activity of similar magnitude.

The detection of amino acids through their optical activity is also the only means to measure by remote sensing the enantiomeric excess in Solar System bodies. Current determinations, based mainly on the analysis of meteorites (Martins and Sephton, 2009), reveal a slight preponderance of L-enantiomers relative to D-enantiomers that reaches as high as $\sim 60\%$ in the analysis of isoleucine series in the Antarctic meteorites (Pizzarello *et al.*, 2012). This asymmetry is observed in all biomolecules on Earth (proteins, sugars, amino acids, RNA, DNA) and could result from the propa-

gation of an originally small imbalance from space amino acids to Earth, suggesting a possible extraterrestrial source.

The source of the enantiomeric excess detected in space bodies is unclear. There are two main accepted models to explain this asymmetry: parity violation by the weak nuclear force or the presence of chiral fields such as circularly polarized light (see Giri *et al.*, 2013). Parity violation can affect molecules by altering the energy levels, introducing energy differences between enantiomers. However, the calculated differences are in the range of 10^{-5} to 10^{-8} erg per mole; as a result, they are very difficult to measure, and it seems highly unlikely that these differences are behind the chirality imbalance in biomolecules (Tranter and McDermott, 1989). On the other hand, laboratory experiments have successfully shown that the enantiomeric balance in racemic mixtures can be broken by irradiation with circularly polarized radiation (CPR). Of special interest are the experiments that use alanine ice under space conditions. The enantiomeric enrichment reached by this procedure is of a few percent and similar to that measured in many meteorites (Meinert *et al.*, 2014).

In this study, we evaluate the detectability of alanine by determining the expected spectropolarimetric signature of comets in our solar system. Our calculations are based on laboratory measurements of the optical activity of alanine and the known properties of comets, in particular, data obtained by the Rosetta probe analysis of the comet 67P/Churyumov-Gerasimenko.

2. Materials and Methods

The structural asymmetry of alanine results in different interactions with left-handed (L) and right-handed (R) circularly polarized radiation (CPR). The most prominent difference can be observed at 180 nm and is usually ascribed to the $\pi_0 \rightarrow \pi^*$ transition of the COO^- group (Kaneko *et al.*, 2009). This optical activity is manifested through two related phenomena: optical rotatory dispersion (ORD) and circular dichroism (CD).

The complex refractive index of alanine, n_C , differs for L- and R-CPR, which can be expressed as $(n_C)_{L,R} = n_{L,R} \pm ik_{L,R}$. This difference is also often expressed in terms of optical constants: $\gamma_1 = \frac{1}{2}(n_L - n_R)$, $\gamma_2 = \frac{1}{2}(k_L - k_R)$, $n = \frac{1}{2}(n_L + n_R)$, $k = \frac{1}{2}(k_L + k_R)$, so $(n_C)_{L,R} = (n \pm \gamma_1) + i(k \pm \gamma_2)$ (Einhorn *et al.*, 1973).

Optical rotatory dispersion is produced by the real component (γ_1 term) and results in a phase lag in the propagation of L-CPR with respect to R-CPR. If the impinging radiation is linearly polarized, ORD produces a rotation, $[\alpha]$, of the plane of polarization such that $[\alpha] = 2\pi\gamma_1(\lambda)/\lambda$ rad cm^{-1} at wavelength λ (with λ in cm).

Circular dichroism is produced by the imaginary component (γ_2 term) and results in different absorbance of L-CPR and R-CPR, which can be denoted as A_L and A_R , respectively. The Beer-Lambert law relates these absorbances to the absorption of radiation:

$$I_{L,R} = I_{L,R}^0 10^{-A_{L,R}} \quad (1)$$

where I^0 and I are the intensities of the incident and transmitted light beams, respectively. The rotation angle can be expressed in terms of the electric field vector as

$$\tan \theta = \frac{I_R^{1/2} - I_L^{1/2}}{I_R^{1/2} + I_L^{1/2}} = \frac{e^{a_0 \Delta A} - 1}{e^{a_0 \Delta A} + 1} \quad (2)$$

with $a_0 = \ln 10/2 = 1.1513$ and $\Delta A = A_L - A_R$. Given the small values involved, $A_{L,R} \ll 1$ and $\tan \theta \approx \theta$; thus,

$$\theta \approx \frac{\ln(10)}{4} \Delta A \quad (3)$$

$A_{L,R}$ can be expressed in terms of the absolute optical absorption coefficient, $\mu_{L,R}$, as $A_{L,R} = \mu_{L,R} \mathcal{Z} / \ln 10 = 0.4343 \mu_{L,R} \mathcal{Z}$, where \mathcal{Z} is the thickness of the medium, usually given in centimeters. Hence,

$$\theta \approx \frac{1}{4} \Delta \mu \mathcal{Z} \quad (4)$$

In a 50%-50% mixture of both isomers, the rotation induced by any one isomer is counterbalanced, resulting in $\theta = 0$. However, mixtures typically are not balanced, either on Earth or in space. Therefore, we can denote l-ala and d-ala as the levo and dextro isomers of alanine and $\Delta \mu^l$ and $\Delta \mu^d$ as the respective absorption coefficients.

$$\theta_{\text{obs}} = \theta^l + \theta^d = 0.25 (\Delta \mu^l + \Delta \mu^d) \mathcal{Z} \quad (5)$$

$\Delta \mu^{l,d}$ can be expressed in terms of the absorption cross section (σ) and the density in terms of molecules per unit volume (n) as

$$\Delta \mu^{l,d} = (\sigma_L^{l,d} - \sigma_R^{l,d}) n^{l,d} \quad (6)$$

where n^l and n^d are the densities of the levo and dextro isomers, respectively. Hence, the total density of alanine is $n = n^l + n^d$, and the fractional abundance of each isomer is $\chi^{l,d} = n^{l,d} / n$. The enantiomeric excess is defined as $ee = (n_l - n_d) / (n_l + n_d) = \chi_l - \chi_d$. Thus, Eq. 5 ($\sigma_{L,R}^l = -\sigma_{L,R}^d$) can be expressed in terms of the enantiomeric excess as

$$\theta_{\text{obs}} = 0.25 \mathcal{Z} (\sigma_L^l - \sigma_R^l) (n^l - n^d) = 0.25 \mathcal{Z} n (\sigma_L^l - \sigma_R^l) ee \quad (7)$$

or, in degrees:

$$\theta_{\text{obs}} (\text{deg}) = 14.3312 \mathcal{Z} n (\sigma_L^l - \sigma_R^l) ee \quad (8)$$

The apparent CD coefficient, $\Delta \mu^l$, was measured by Kaneko *et al.* (2009) on a film having the density $\rho = 1.42 \text{ g cm}^{-3}$ and is included in Eq. 9:

$$\begin{aligned} (\sigma_L^l - \sigma_R^l) (\text{cm}^2) &= \frac{\Delta \mu^l (\text{cm}^{-1}) 89.09 (\text{g})}{\rho (\text{g cm}^{-3}) N_A} \\ &= 1.0417 \times 10^{-22} \Delta \mu^l (\text{cm}^{-1}) \end{aligned} \quad (9)$$

which includes the molar mass of alanine (89.09) and N_A , Avogadro's constant. Thus,

$$\theta_{\text{obs}} (\text{mdeg}) = 1.4928 \times 10^{-18} \mathcal{Z} (\text{cm}) n (\text{cm}^{-3}) \Delta \mu^l (\text{cm}^{-1}) ee \quad (10a)$$

The strength of the circular polarization signal is given by the Stokes V parameter defined as $V = I_R - I_L = I_0 \ln 10 \Delta A = 4I_0 \theta$. Hence,

$$V = 1.0422 \times 10^{-22} \mathcal{Z} (\text{cm}) n (\text{cm}^{-3}) \Delta \mu^l (\text{cm}^{-1}) ee I_0 \quad (10b)$$

This calculation has been carried taking into account the different absorbance to L-CPR and R-CPR by the two enantiomers, and as such it assumes that the radiation impinging the sample is circularly polarized. However, it is not required that the comet outgassing is irradiated by CPR to detect the CD signature of a non-racemic mixture, since such a mixture acts as a polarizer by itself. The induced fractional circular polarization of unpolarized incident light, or induced polarizance, is comparable in magnitude to the differential absorbance computed in Eq. 10a. This technique has been successfully used in the lab to detect photosynthetic microbes (Sparks *et al.*, 2009a) and to study *in vivo* structural variations of plant and algae chloroplast (Patty *et al.*, 2017), and it is also the reason to consider the detection of CPR as a possible biomarker (Sparks *et al.*, 2009b).

2.1. Expected signals in cometary spectra

The 140–250 nm spectrum of comets is characterized by a weak continuum produced by scattering of solar radiation and several prominent emission lines. Among these, CI (156.1, 161, 165.7 nm) and SI (142.5, 147.3, 180.7 nm) predominate, and CS (0,0) and CO⁺ bands are also present (Fig. 1). The location of the CO Cameron bands that are prominent in comets is also indicated for reference.

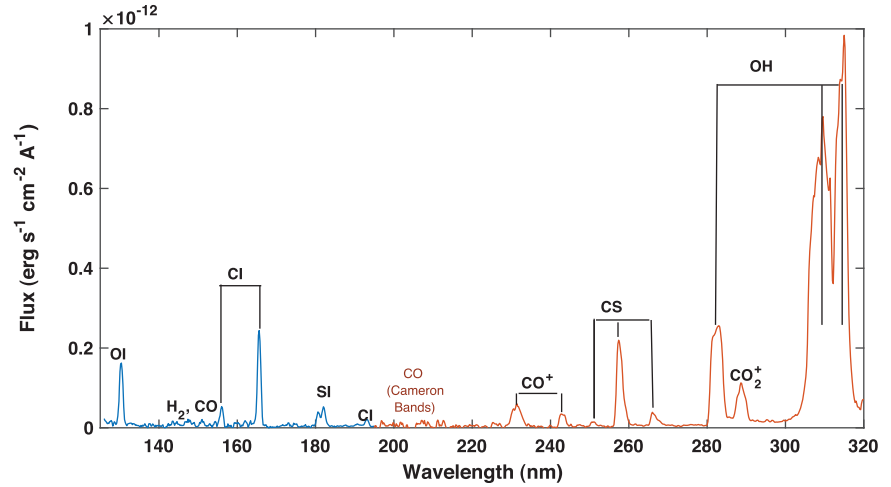
Radiation from comets is polarized both linearly and circularly (Hines and Levasseur-Regourd, 2016; Rosenbush *et al.*, 2007). The linear polarization at optical wavelengths may be as high as 25%, especially at large phase angles, and decreases approaching the UV range (Hines and Levasseur-Regourd, 2016). Extrapolating from optical data results in expected values of about 7% at 180 nm for phase angles of 40° to 60° (Kiselev *et al.*, 2008). Circular polarization in the optical ranges is around ~1% and can be produced by several mechanisms, including multiple scattering in asymmetric particle distributions and scattering by intrinsically asymmetric particles that may (Nagdimunov *et al.*, 2013) or may not (Guirado *et al.*, 2007) be organic. However, the CD signature of a given amino acid is observed in a narrow spectral band and provides conclusive identification of the molecule that can be further confirmed by ORD detection and the Cotton effect (see, *e.g.*, the UV spectral signature of CD for various amino acids in Meierhenrich *et al.* [2010], Fig. 1). Both CD and ORD can be related through the Kramers-Kronig relation:

$$[\alpha](\lambda) = 2.1018 \times 10^3 \int_0^\infty \Delta \mu(\lambda') \frac{\lambda'^2}{\lambda^2 - \lambda'^2} d\lambda' \quad (11)$$

Note that the ORD is significantly stronger than the CD and approaches 0 at the central wavelength of the CD band; this is the so-called Cotton effect.

To evaluate the CD signal expected from comets, the number of molecules along the optical path must be determined. Although no measurement of the abundance of

FIG. 1. UV spectrum of comet Bradley as observed by the International Ultraviolet Explorer (IUE) in 1980 (Weaver *et al.*, 1981). The main spectral features are marked, including the location of the Cameron CO bands that are not observed in IUE data. The OH feature is saturated in the image. The continuum produced by comet-induced solar radiation scattering is very weak. The comet was at heliocentric distance 0.71 and 0.61 AU from the IUE (Feldman *et al.*, 1980). Color images are available online.



alanine in comets is yet available, this value can be inferred from the expected abundance of alanine relative to glycine, $n_{\text{ala}}/n_{\text{gly}} \sim 0.4$ based on laboratory experiments (Muñoz Caro *et al.*, 2002).

Glycine has been detected in the coma of comet 67P/Churyumov-Gerasimenko by the ROSINA mass spectrometer in the Rosetta probe (Altwegg *et al.*, 2016). ROSINA detected glycine in the gas phase released from sublimation of the icy mantles of dust grains in the coma, and an abundance of 170 ppb was derived (Hadraoui *et al.*, 2019). The density and thickness of the glycine cloud can be expressed as $n_{\text{gly}} = 2.1 \times 10^7 \text{ cm}^{-3}$ and $L_{\text{gly}} = 2 \times 10^6 \text{ cm}$. We introduced these values into Eqs. 12a and 12b:

$$\theta_{\text{obs}}(\text{arcsec}) = 0.0903 \left(\frac{Z}{2 \times 10^6 \text{ cm}} \right) \left(\frac{n}{8.4 \times 10^6 \text{ cm}^{-3}} \right) \left(\frac{\Delta\mu^l}{10^3 \text{ cm}^{-1}} \right) ee \quad (12a)$$

$$V = 1.7509 \times 10^{-6} \left(\frac{Z}{2 \times 10^6 \text{ cm}} \right) \left(\frac{n}{8.4 \times 10^6 \text{ cm}^{-3}} \right) \left(\frac{\Delta\mu^l}{10^3 \text{ cm}^{-1}} \right) ee I_0 \quad (12b)$$

Enantiomeric excesses in meteorites range between 1% and 10% (Pizzarello and Cronin, 2000), reaching as high as ~60% in the isoleucine series in Antarctic meteorites (Pizzarello *et al.*, 2012). In Fig. 2, V is represented for $ee=10\%$ and two plausible I_0 spectral distributions: the International Ultraviolet Explorer (IUE) spectrum for the Bradley comet (as per Fig. 1) and the scattered solar spectrum in a body with UV albedo 0.05 that was observed under the same conditions. The solar spectrum was retrieved from the Hubble telescope database¹ of spectrophotometric standards, multiplied by the albedo and rescaled based on assumed radiation from a surface having a 50 km radius, at a heliocentric distance of 0.71 AU observed from a satellite

0.61 AU from the body, that is, under the same observing conditions as used for comet Bradley. This spectrum is denoted as SunS in the text. V is represented for $ee=+0.1$ (a 10% of l-ala excess) and $ee=-0.1$ (a 10% of d-ala excess) to highlight wavelengths at which the CD changes sign. Comparison between the comet and SunS spectra shows higher likelihood of detectability in comets, particularly those having very strong OI (130 nm) and SI (180 nm) features.

The icy mantles of the grains also contribute to the CD signal. The dust-to-gas mass ratio in the 67P/Churyumov-Gerasimenko coma is ~ 3 (Rotundi *et al.*, 2015), and the H_2O ice mass fraction of the dust particles is ~ 1 (Hadraoui *et al.*, 2019). Hence, Eqs. 12a and 12b provide a lower limit for the expected signal, and observed values could increase by a factor of 4 due to the contribution of alanine present in the icy grains. The contribution from back-scattered (*i.e.*, reflected) radiation to the CD signal is negligible in this context (Einhorn *et al.*, 1973; Silverman and Badoz, 1990).

To evaluate the strength of the alanine ORD signal, Eq. 11 was integrated numerically, and $\Delta\mu^l$ in the 180 nm band was subjected to Gaussian fitting to facilitate the integration. When

$$I^l(\lambda) = \int_0^\infty \Delta\mu^l \frac{\lambda^2}{\lambda'^2 - \lambda^2} d\lambda \quad (13)$$

the total rotatory effect will depend on the enantiomeric excess such that

$$\alpha_{\text{obs}} = \alpha^l - \alpha^d = Zn[\alpha^l] \frac{89.09 \text{ (g)}}{\rho \text{ (g cm}^{-3}) N_A} ee \quad (14)$$

and the expected rotation of the plane of polarization induced by alanine is

$$\alpha_{\text{obs}}(\text{arcmin}) = 2.5280 \left(\frac{Z}{2 \times 10^6 \text{ cm}} \right) \left(\frac{n}{8.4 \times 10^6 \text{ cm}^{-3}} \right) \left(\frac{I^l(\lambda)}{200} \right) ee \quad (15)$$

¹<https://eso.org/sci/observing/tools/standards/spectra/hststandards.html>

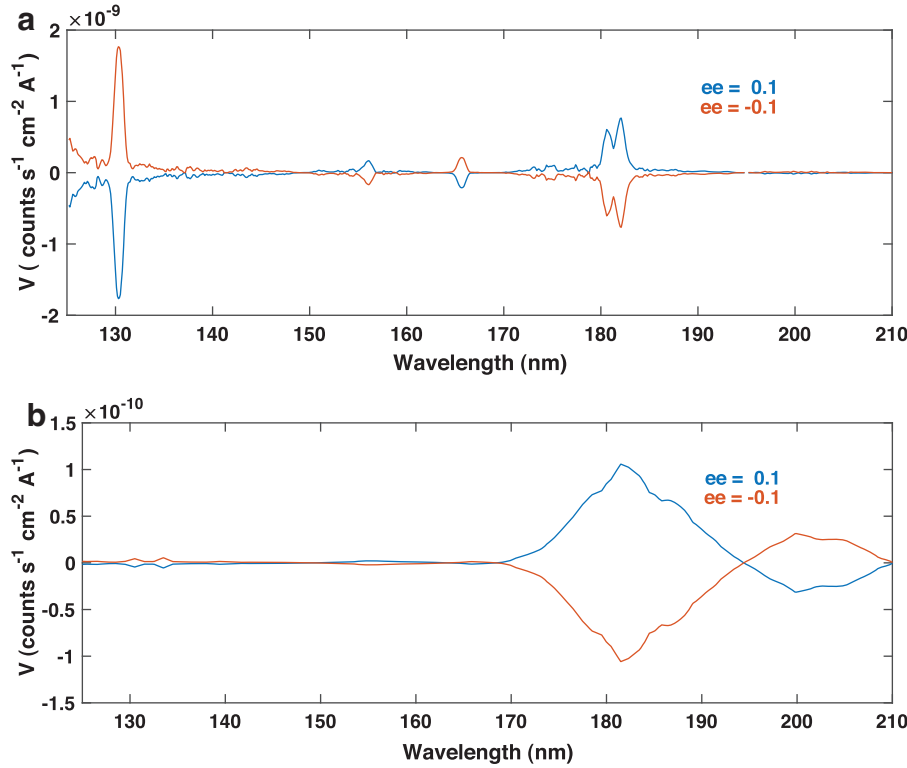


FIG. 2. (a) Stokes V parameter for comet Bradfield at $ee=0.1$ and $ee=-0.1$ in blue and red, respectively. The IUE spectrum of comet Bradfield in Fig. 1 was used for calculation. (b) Stokes V parameter for the SunS spectrum (see text). In the plot, $ee=0.1$ and $ee=-0.1$ are represented in blue and red, respectively. Color images are available online.

In terms of the Stokes parameters U and Q ,

$$\tan(2\alpha_{\text{obs}}) = \frac{U}{Q} \quad (16)$$

and, as $\alpha_{\text{obs}} \ll 1$,

$$2\alpha_{\text{obs}} = 1.47 \times 10^{-3} \left(\frac{Z}{2 \times 10^6 \text{cm}} \right) \left(\frac{n}{8.4 \times 10^6 \text{cm}^{-3}} \right) \left(\frac{I^l(\lambda)}{200} \right) ee \quad (17)$$

α_{obs} is displayed in Fig. 3 for $ee=0.1$ and compared with comet Bradley and SunS spectral energy distributions. The maximum rotation was observed in a featureless area of the cometary spectra.

The rotation angle depends linearly on the number of alanine molecules along the line of sight (on Z and n), thus, the higher the concentration of the molecule the better the chance of detection. Carrying out spectropolarimetric observations has the advantage of recording simultaneously the polarization at the alanine feature and at unaffected nearby wavelengths; as a result, variation of the polarization strength and orientation which are characteristics of cometary environments can be properly corrected.

3. Discussion: Requirements for Remote Detection of Alanine in Comets

Section 2 showed that the expected signal from alanine in the UV spectrum is very low. In terms of Stokes parameters and for $ee=0.1$:

$$V = 1.75 \times 10^{-7} I_0 \quad (18)$$

$$\frac{U}{Q} = 1.47 \times 10^{-4}$$

Measurement of Stokes parameters thus requires design of an instrument that is outside the scope of this study (see Azzam, 2016, for a review of the current status of instruments to measure the four Stokes parameters). However, an order-of-magnitude estimate is feasible based on simple, widely available designs. A common setup consists of a rotating waveplate that acts as polarizer and a Wollaston prism that splits the beam into two orthogonal linear polarization states (Pertenais *et al.*, 2017). In this modulation-detection scheme, the beam passes through a waveplate with retardance δ while rotating at an angular frequency, Ω , and is split by the Wollaston prism into ordinary and extraordinary beams. The two beams are then projected on the detector, and the difference between the signals is measured at discrete intervals of the phase Ωt , that is, the waveplate orientation. Assuming that both channels are perfectly balanced, the difference in the intensity between the simultaneous output of the channels can be expressed as

$$Q = \frac{1}{2} [1 + \cos \delta + (1 - \cos \delta) \cos 4\Omega t] \quad (19)$$

$$U = \frac{1}{2} (1 - \cos \delta) \sin 4\Omega t$$

$$V = -\sin \delta \sin 2\Omega t$$

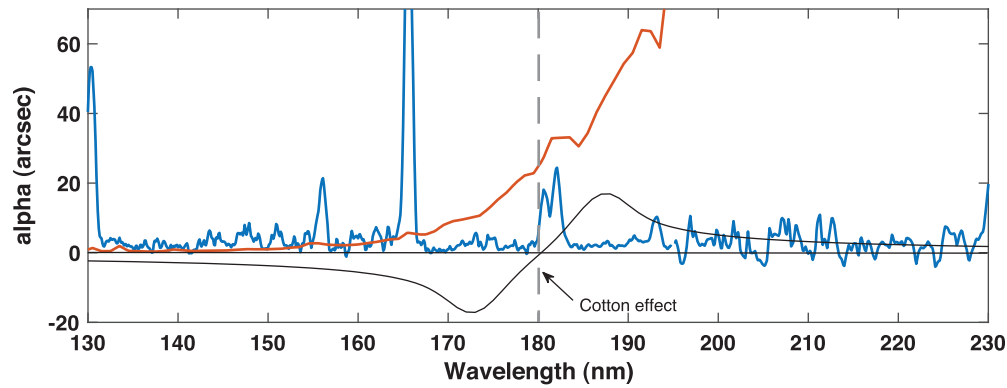


FIG. 3. α_{obs} for $ee=0.1$ (black). Comet Bradley (blue) and SunS (red) energy distribution in the relevant wavelength range is shown in arbitrary units. Color images are available online.

where Q , U , and V are periodic signals of known period. Thus, signal pollution by other effects such as telescope jittering can be corrected. Indeed, strategies for optimal modulation are well studied in the context of solar spectropolarimetric measurements, which are also challenging to acquire (Lites, 1987; del Toro Iniesta and Collados, 2000). For the low signals associated with alanine detection, many Ω cycles will need to be combined to reach the limit of detection. The number of cycles, that is, the total exposure time, is determined by the collecting capacity of the telescope, the efficiency of the instrumentation, and the distance to the comet.

If the major source of noise is photon noise ($\propto N_{\nu}^{1/2} = (I_0/h\nu)^{1/2}$), a simple estimate of the signal to noise ratio (SNR) required to detect V at 3σ level is $\text{SNR} = V/N_{\nu}^{1/2} = 3$, and from Eq. 12b,

$$3 = 1.7509 \times 10^{-6} \left(\frac{Z}{2 \times 10^6 \text{cm}} \right) \left(\frac{n}{8.4 \times 10^6 \text{cm}^{-3}} \right) \left(\frac{\Delta \mu^l}{10^3 \text{cm}^{-1}} \right) ee(N_{\nu})^{1/2} \quad (20)$$

TABLE 2. IUE SPECTRA

Comet	Year observed	IUE archive image ID	Heliocentric distance*	Distance to IUE*
Bradfield	1980	SWP07624	0.71	0.61
		SWP07625		
Halley	1986	SWP27884	0.84	1
		SWP27898	0.87	1.02
		SWP27906	0.89	0.99
		SWP27908	0.90	0.96
		SWP27914	0.92	0.94
Levy	1990	SWP39629	1.18	0.76
		SWP39656	1.13	0.84
		SWP39658	1.13	0.85
Austin	1990	SWP38750	0.83	0.42
Swift-Tuttle	1992	SWP46279	1.062	1.20
		SWP46320	1.01	1.27
Hyakutake	1996	SWP56904		
		SWP56906		
		SWP56907		

*Heliocentric distance and distance to Earth were retrieved from Festou (1990), Feldman *et al.* (1997), and Tozzi *et al.* (1998).

where N_{ν} depends on the temporal sampling in Eq. 19, the number of combined cycles, the collecting capability of the telescope, and the instrument configuration. A standard configuration for space observatories involves a Ritchey-Chretien mounting telescope that feeds the spectropolarimeter. A simple spectropolarimeter can comprise a polarizer, reflection grating with a spectral dispersion of 600 in the 130–250 nm spectral range, and an MCP-type photon counting detector². In the spectral range of interest, the transmittance of this optical system with standard UV coatings and components is about 15%, and the QE of a Cs_2Te detector is 35% (Carruthers, 2000). This configuration is similar to that of the Ultraviolet Researcher for the Investigation of the Emergence of Life mission (URIEL) submitted to the ESA call for F-missions (Gómez de Castro *et al.*, 2020).

N_{ν} also depends on the characteristics of the comet and the distance between the comet and the Sun. To adequately sample the expected UV flux from comets, all available observations from the archives of the IUE and the Hubble Space Telescope (HST) with the instruments Space Telescope Imaging Spectrograph (STIS) and Cosmic Origins Spectrograph (COS) have been analyzed. The IUE obtained good quality spectra from the Bradfield (1980), Halley (1986), Levy (1990), Swift-Tuttle (1992), and Hyakutake (1996) comets. HST/STIS spectra are available for Hartley 2, Hale-Bopp, Lee, Linear, 2000WM1, Borelly, Ikeya-Zhang, Neat 2001-Q4, C2009-P1 Garradd-New, and Lovejoy comets. Good HST/STIS observations were obtained with grating G230L that covers the spectral range 157–318 nm, but unfortunately the signal is low and noisy in the 150–200 nm region where alanine features are observed. HST/COS observations are also very poor in this region. Hence, only IUE data were used for this study (Table 2).

Using these parameters, we calculated the distance comet–space telescope, d , required to reach $\text{SNR}=3$ in a total observing time, T_{obs} , of 10 days in which continuous observation was conducted with telescopes having a primary mirror with diameter ranging from 50 cm (explorer size) to the 1500 cm of LUVUOIR-A.

²Photon noise is the main source of noise in UV spectroscopic measurements using MCP-type detectors.

$$d = \frac{1.7509 \times 10^{-6}}{3} \left(\frac{Z}{2 \times 10^6 \text{ cm}} \right) \left(\frac{n}{8.4 \times 10^6 \text{ cm}^{-3}} \right) \left(\frac{\Delta\mu^1}{10^3 \text{ cm}^{-1}} \right) ee (T_{\text{obs}} N_{\nu})^{1/2} D \quad (21)$$

Circular dichroism is measured by integrating the signal received in the 174.5–189.6 nm spectral range. In Fig. 4a, the observing distance is represented as a function of the diameter of the telescope primary mirror for $ee=0.01$, 0.1, and 1. Clearly, even under the ideal conditions of this calculation, the signal detected by an astronomical observatory using current technology is very low: about 2 counts in V for a Hubble-type telescope and the observation con-

ditions described above. Increasing this value by a factor of 10 seems feasible with the ongoing technical advancements for the future UV missions (see Gómez de Castro *et al.* [2021] for a recent review). Moreover, small instruments would be able to detect the CD signature if flown near comets or asteroids. A small mission navigating the asteroid belt could thus provide significant insight into alanine abundance.

The ORD signal is significantly stronger and is measured based on the ratio of two Stokes parameters, U and Q . For an expected percentage linear polarization $p=(Q^2 + U^2)^{1/2}/I=0.07$ for the 180 nm feature (see above), a total beam intensity of I_0 and noise $N_{\nu}^{1/2}$, the error in measurement at position angle, θ , is given by

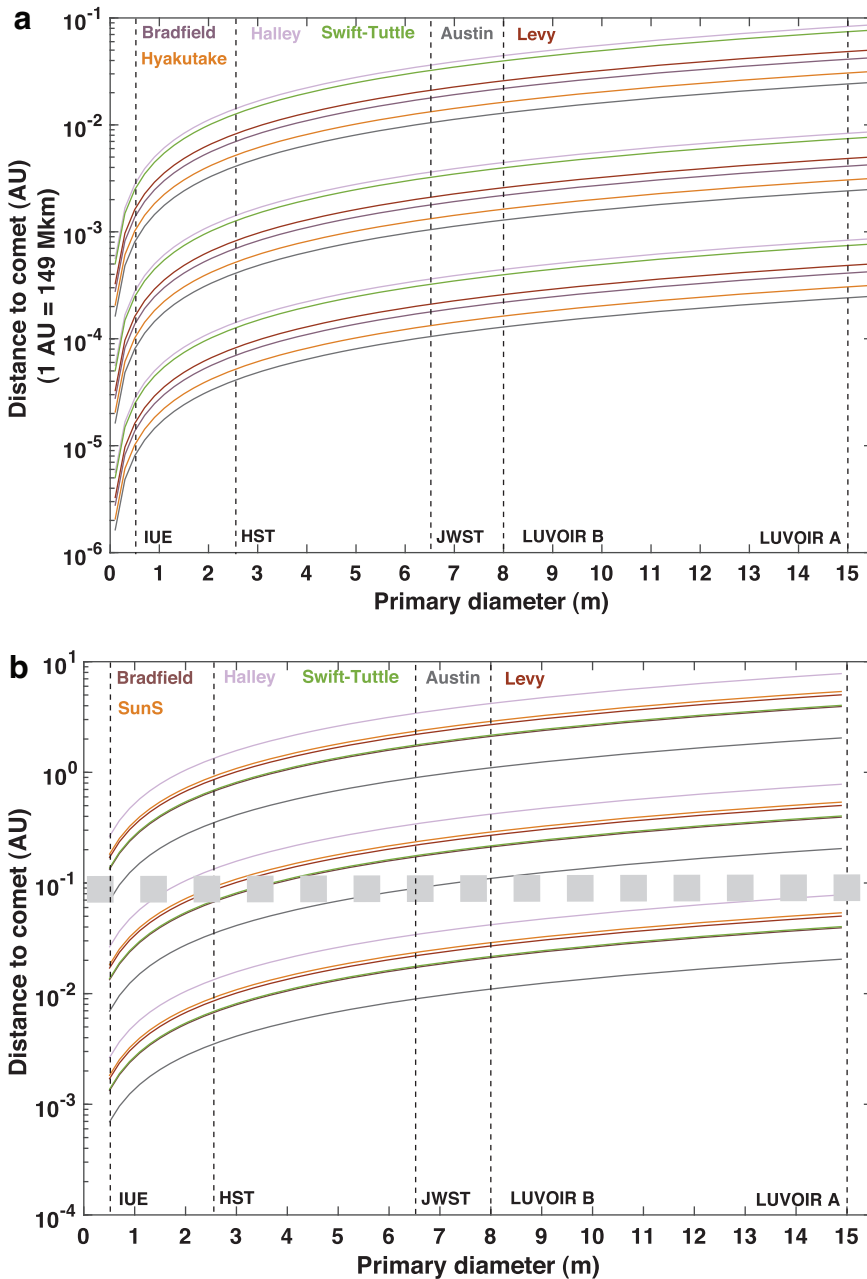


FIG. 4. (a) Detectability of alanine CD signal at $ee=1$, 0.1, and 0.01 (top, middle, and bottom sets of curves). The distance to the comet required to reach $\text{SNR}=3$ (see text) is plotted against the primary mirror diameter of the telescope. The diameters of the primary mirrors of reference space telescopes are indicated. The curves were calculated based on IUE spectra (Table 2) for Halley, Swift-Tuttle, Austin, Bradfield, Levy, and Hyakutake comets (see text). (b) Detectability of alanine ORD signal for $ee=1$, 0.1, and 0.01 (top, middle, and bottom sets of curves). The distance to the comet required to reach $\text{SNR}=3$ (see text) is plotted against the primary mirror diameter of the telescope. The diameters of the primary mirrors of reference space telescopes are indicated. The curves were calculated based on IUE spectra (Table 2) of Halley, Swift-Tuttle, Austin, Bradfield, and Levy comets and the SunS spectrum (see text). The thick dashed line marks a distance of 0.1 AU and represents the boundary for detectability by remote detection with a space observatory; the likelihood of many comets to pass within 0.1 AU is low. Color images are available online.

$$\delta\theta = \frac{1}{2} \frac{N_\nu^{-1/2}}{0.07} \quad (22)$$

For ORD to be detected conclusively, $\alpha_{\text{obs}} \geq 3 \delta\theta$, or

$$0.74 \times 10^{-3} \left(\frac{Z}{2 \times 10^6 \text{cm}} \right) \left(\frac{n}{8.4 \times 10^6 \text{cm}^{-3}} \right) \left(\frac{I^1(\lambda)}{200} \right) ee \geq 3 \frac{1}{2} \frac{N_\nu^{-1/2}}{0.07} \quad (23)$$

Hence,

$$d = 3.45 \times 10^{-5} \left(\frac{Z}{2 \times 10^6 \text{cm}} \right) \left(\frac{n}{8.4 \times 10^6 \text{cm}^{-3}} \right) \left(\frac{I^1(\lambda)}{200} \right) ee N_\nu^{1/2} D \quad (24)$$

In Fig. 4b, the distance of the comet to the space probe is plotted against the size of the telescope's primary mirror

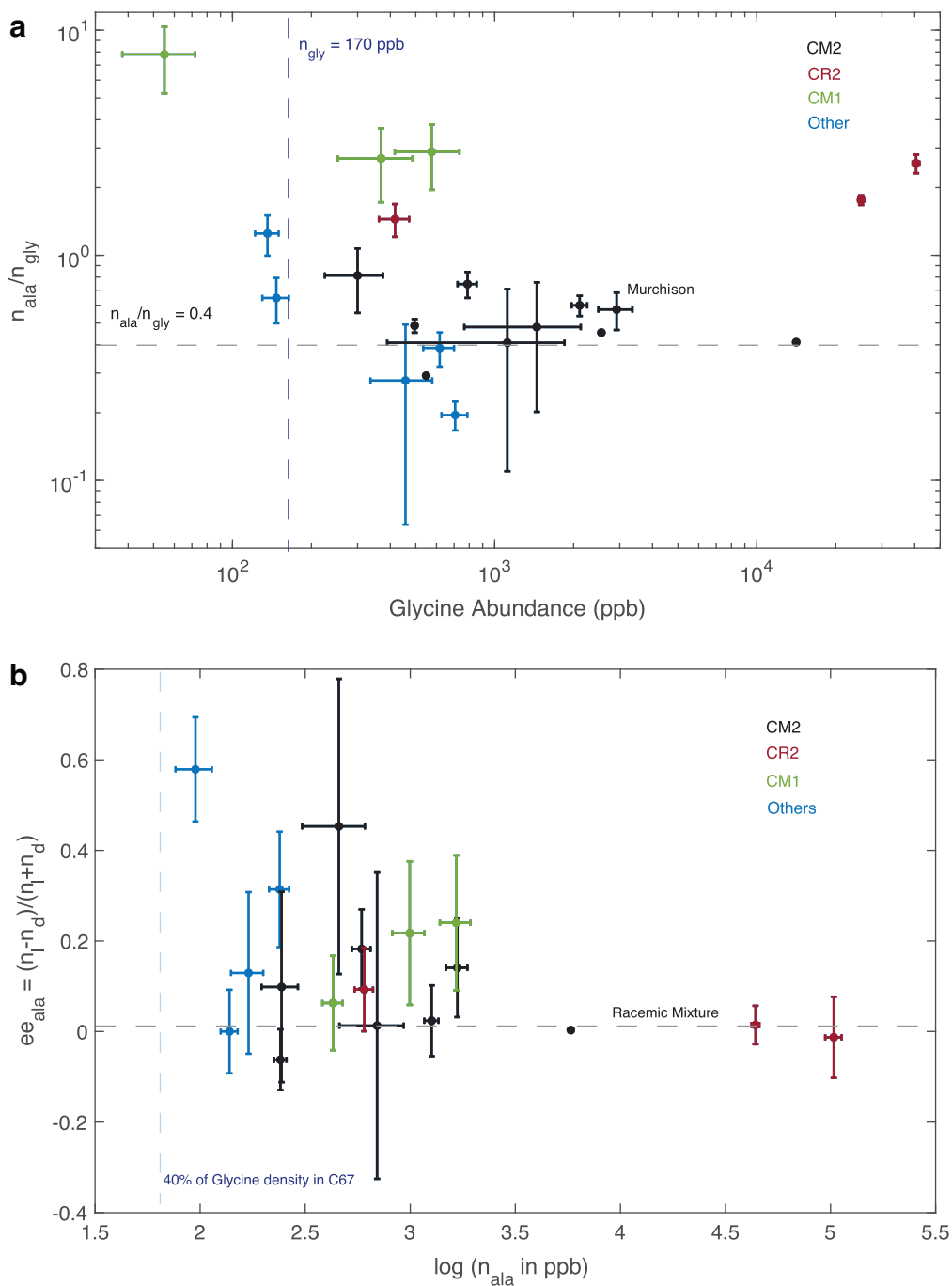


FIG. 5. Top: Characteristics of the alanine content in carbonaceous chondrites. Alanine to glycine abundance against the glycine abundance. Bottom: Enantiomeric excess against alanine abundance. Color images are available online.

under the same assumptions as for CD. The main conclusions based on this plot are as follows:

- (i) Measuring the ORD is achievable for $ee=1$ even for observatories with telescopes having small (*e.g.*, 50 cm) primary mirrors, and the low density of the 67P/Churyumov-Gerasimenko coma.
- (ii) Reaching $ee=0.1$ is achievable for the brightest comets using medium-sized space telescopes, but large telescopes are needed to observe the weakest objects.
- (iii) Detection of very low ee (≤ 0.01) is not feasible by remote observation, although small spectropolarimeters in exploration missions (*e.g.*, Rosetta) can be used for remote detection of alanine in a comet without sample procurement.
- (iv) The signal from the SunS spectrum is detectable. This is the expected backscattered spectrum from small icy bodies and opens the possibility of studying numerous minor bodies especially, after collisions when alanine will be released from the ice into the gas phase.

4. Conclusions and Implications

In this study, we have calculated the expected strength of the optical activity signatures (CD and ORD) of alanine in Solar System comets. The calculations are based on the only available measurement of the abundance of glycine in a comet. These estimates are conservative; while glycine abundance is 170 ppb in comet 67P/Churyumov-Gerasimenko, it is well known that it may rise to few thousands in chondrites with aqueous alteration (Martins and Sephton, 2009). In fact, ROSINA measurements indicate that C67/Churyumov-Gerasimenko is built of rather pristine material that has not been significantly altered either by heat or liquid water. However, this is not going to be the most generic case. In Fig. 5, we have plotted the $n_{\text{ala}}/n_{\text{gly}}$ and the alanine enantiomeric excess (ee) of well-studied carbonaceous chon-

drites (Martins and Sephton, 2009); it is clear from the figure that both alanine abundance varies by several orders of magnitude from one sample to another and that measurements from comet 67P/Churyumov-Gerasimenko are in the low-abundance end. In Fig. 6, we display the expected values of the ratios V/I and U/Q between the Stokes parameters for the set of abundances and ee 's in Fig. 5. The vast majority of the data are well above the fiducial values used for the calculations in Fig. 4a, 4b with $ee=0.1$, and as expected the very hydrated chondrites (CM1, CM2) are more than 1 order of magnitude above. In spite of this, the CPR signal (V/I) is very small and cannot be measured by remote observation with current technology, as extensively discussed in Section 3. However, remote detection of alanine by ORD is clearly feasible.

Alanine is not the only chiral amino acid expected to be formed in cometary environments; other amino acids are synthesized in laboratory experiments carried out with space ices, among them serine, valine, or proline (Muñoz Caro *et al.*, 2002). All of them display features at wavelengths between 140 and 270 nm with very different spectral signatures in terms of the center and width of the band, the precise shape and strength (see, *e.g.*, Fig. 1 in Meierhenrich *et al.*, 2010); however, their detection will require even most sensitive instrumentation. The main challenge for the detection of amino acids is the weakness of the signal detected from Earth that requires an optimization of the optical system as well as making use of optimal observation conditions: observation of the brightest parts of the comets such as the head instead of the coma and observation at the smallest heliocentric and geocentric distances possible.

Alanine detection will depend on the imbalance in abundance between the two enantiomers. Measuring whether L-alanine in comets is the most abundant isomer, as it is on Earth, is a challenging, but feasible, task according to the calculations described in this study.

The advantage of remote sensing over direct measurements is clear in terms of both cost and opportunity. The heliocentric distance of the comets observed by the IUE

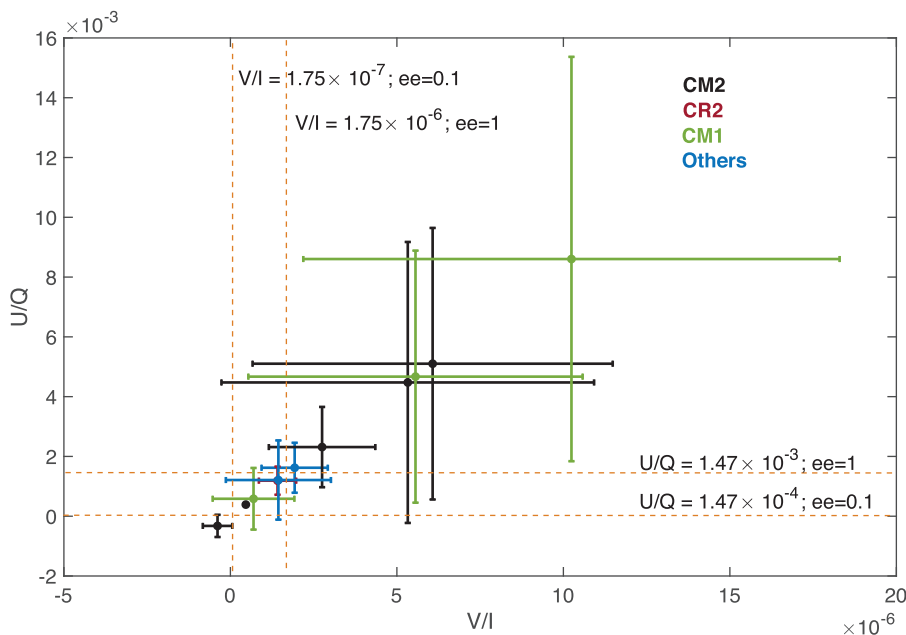


FIG. 6. V/I and U/Q derived from known alanine abundances and alanine enantiomeric excess in the carbonaceous chondrites represented in Fig. 5. The dotted yellow lines represent the values of V/I and U/Q used for the detectability calculations in Fig. 4a, 4b. Color images are available online.

mission, as well as their distance to the satellite, is known (Table 2; Festou, 1990). Remote sensing of comets will provide sufficient statistical power to draw conclusions about whether enantiomeric imbalances are common in the Solar System to $\epsilon > 0.1$. Meanwhile, small instruments aboard planetary probes can provide fundamental information to map the origin and distribution routes of amino acids in the Solar System.

Acknowledgments

This research is funded in part by the Ministry of Science and Innovation of Spain under grant ESP2017-87813-R. A.I. Gómez de Castro thanks Federico Morán, Juli Pereto, Uwe Meierhenrich, and very especially Søren Vrønning Hoffmann for enlightening discussions.

References

- Altwegg, K., Balsiger, H., Bar-Nun, A., *et al.* (2016) Prebiotic chemicals—amino acid and phosphorus—in the coma of comet 67P/Churyumov-Gerasimenko. *Sci Adv* 2:e1600285.
- Ayres, T.R., Fleming, T.A., Simon, T., Haisch, B.M., Brown, A., Lenz, D., Wamsteker, W., de Martino, D., Gonzalez, C., Bonnell, J., *et al.* (1995) The RIASS Coronathon: joint X-ray and ultraviolet observations of normal F–K stars. *Astrophys J Suppl Ser* 96, doi:10.1086/192118.
- Azzam, R.M.A. (2016) Stokes-vector and Mueller-matrix polarimetry. *J Opt Soc Am A Opt Image Sci Vis* 33:1396–1408.
- Bernstein, M.P., Dworkin, J.P., Sandford, S.A., Cooper, G.W., and Allanadola, L.J. (2002) Racemic amino acids from the ultraviolet photolysis of interstellar ice analogues. *Nature* 416:401–403.
- Carruthers, G.R. (2000) Ultraviolet and X-ray detectors. In *Electro-Optics Handbook*, 2nd ed., edited by R.W. Waynant and M.N. Ediger, McGraw-Hill, New York, Chapter 15.
- Chen, Y.-J., Nuevo, M., Yih, T.-S., Ip, W.-H., Fung, H.-S., Cheng, C.-Y., Tsai, H.-R., and Wu, C.-Y.R. (2008) Amino acids produced from the ultraviolet/extreme-ultraviolet irradiation of naphthalene in a H₂O+NH₃ ice mixture. *Mon Not R Astron Soc* 384:605–609.
- Cleaves, H.J., Chalmers, J.H., Lazcano, A., Miller, S.L., and Bada, J.L. (2008) A reassessment of prebiotic organic synthesis in neutral planetary atmospheres. *Orig Life Evol Biosph* 38:105–115.
- del Toro Iniesta, J.C., and Collados, M. (2000) Optimum modulation and demodulation matrices for solar polarimetry. *Applied Optics* 39:1637–1642.
- Draine, B. (1978) Photoelectric heating of interstellar gas. *Astrophys J Suppl Ser* 36, doi:10.1086/190513.
- Einhorn, A.J., Phelps, F.W., and Pao, Y.-H. (1973) Reflection spectroscopy of optically active materials. *Chem Phys* 1:277–296.
- Feldman, P.D., Weaver, H.A., Festou, M.C., A'Hearn, M.F., Jackson, W.M., Donn, B., Rahe, J., Smith, A.M., and Benvenuti, P. (1980) IUE observations of the UV spectrum of comet Bradfield. *Nature* 286:132–135.
- Feldman, P.D., Festou, M.C., Tozzi, G.P., and Weaver, H.A. (1997) The CO₂/CO abundance ratio in 1P/Halley and several other comets observed by IUE and HST. *Astrophys J* 475, doi:10.1086/303553.
- Festou, M.C. (1990) *IUE Access Guide No. 2: Comets*, SP-1134, ESA Publications Division, ESTEC, Noordwijk, the Netherlands.
- Gómez de Castro, A.I., and Marcos-Arenal, P., (2012) Extended magnetospheres in pre-main-sequence evolution: from T Tauri stars to the brown dwarf limit. *Astrophys J* 749, doi:10.1088/0004-637X/749/2/190.
- Gómez de Castro, A.I., Bacciotti, F., Beitia-Antero, L., *et al.* (2020) The Ultraviolet Researcher for the Investigation of the Emergence of Life. On-line Proceedings of the 5th NUVA workshop; <https://www.nuva.eu/scientific-program-virtual/>
- Gómez de Castro, A.I., Barstow, M. A., Brosch, N., *et al.* (2021) UV facilities for the investigation of the origin of life. In *UV Astronomy and the Quest for the Origin of Life*; edited by A.I. Gómez de Castro, Elsevier.
- Guirado, D., Hovenier, J.W., and Moreno, F. (2007) Circular polarization of light scattered by asymmetrical particles. *Journal of Quantitative Spectroscopy and Radiative Transfer* 106:63–73.
- Hadraoui, K., Cottin, H., Ivanovski, S.L., Zapf, P., Altwegg, K., Benilan, Y., Biver, N., Della Corte, V., Fray, N., Lasue, J., *et al.* (2019) Distributed glycine in comet 67P/Churyumov-Gerasimenko. *Astron Astrophys* 630, doi:10.1051/0004-6361/201935018.
- Hines, D.C., and Levasseur-Regourd, A.-C. (2016) Polarimetry observations of comets: status, questions, future pathways. *Planet Space Sci* 123:41–50.
- Kaneko, K., Yagi-Watanabe, K., Tanaka, M., and Nakagawa, K. (2009) Natural circular dichroism spectra of alanine and valine films in vacuum ultraviolet region. *Journal of the Physical Society of Japan* 78, doi:10.1143/JPSJ.78.013001.
- Kiselev, N., Rosenbush, V., Kolokolova, L., and Antonyuk, K.A. (2008) The anomalous spectral dependence of polarization in comets. *J Quant Spectrosc Radiat Transfer* 109: 1384–1391.
- Lites, B.W. (1987) Rotating waveplates as polarization modulators for Stokes polarimetry of the sun: evaluation of seeing-induced crosstalk errors. *Applied Optics* 26:3838–3845.
- Loeb, A., Batista, R.A., and Sloan, D. (2016) Relative likelihood for life as a function of the cosmic time. *Astrophys J Lett* 819, L21.
- Martins, Z., and Sephton, M.A. (2009) Extraterrestrial amino acids. In *Amino Acids, Peptides and Proteins in Organic Chemistry. Vol.1: Origins and Synthesis of Amino Acids*, edited by A.B. Hughes, Wiley-VCH Verlag GmbH & Co. KGaA, Weinheim; pp 3–41.
- Martins, Z., Botta, O., Fogel, M.L., Sephton, M.A., Glavin, D.P., Watson, J.S., Dworkin, J.P., Schwartz, A.W., and Ehrenfreund, P. (2008) Extraterrestrial nucleobases in the Murchison meteorite. *Earth Planet Sci Lett* 270:130–136.
- Meierhenrich, U.J., Filippi, J.-J., Meinert, C., Bredehöft, J.H., Takahashi, J.-i., Nahon, L., Jones, N.C., and Hoffmann, S.V. (2010) Circular dichroism of amino acids in the vacuum-ultraviolet region. *Angew Chem Int Ed Engl* 49: 7799–7802.
- Meinert, C., Hoffmann, S.V., Cassam-Chenai, P., Evans, A.C., Giri, C., Nahon, L., and Meierhenrich, U.J. (2014) Photonenergy-controlled symmetry breaking with circularly polarized light. *Angew Chem Int Ed Engl* 53:210–214.
- Miller, S.L. (1953) Production of amino acids under possible primitive Earth conditions. *Science* 117:528–529.
- Miller, S.L., and Urey, H.C. (1959) Organic compound synthesis on the primitive Earth. *Science* 130:245–251.
- Muñoz Caro, G.M., Meierhenrich, U.J., Schutle, W.A., Barbier, B., Arcones Segovia, A., Rosenbauer, H., Theimann, H.-P., Brack, A., and Greenberg, J.M. (2002) Amino acids from ultraviolet irradiation of interstellar ice analogues. *Nature* 416:403–406.

- Nagdimunov, L., Kolokolova, L., and Mackowski, D. (2013) Characterization and remote sensing of biological particles using circular polarization. *J Quant Spectrosc Radiat Transf* 131:59–65.
- Oró, J. (1967) Stages and mechanisms of prebiological organic synthesis. In *Origins of Prebiological Systems and of Their Molecular Matrices*, edited by S.W. Fox, Academic Press, New York, pp 137–171.
- Parker, E.T., Cleaves, H.J., Dworkin, J.P., Glavin, D.P., Callahan, M., Aubrey, A., Lazcano, A., and Bada, J.L. (2011) Primordial synthesis of amines and amino acids in a 1958 Miller H₂S-rich spark discharge experiment. *Proc Natl Acad Sci USA* 108:5526–5531.
- Patty, C.H.L., Visser, L.J.J., Ariese, F., Buma, W.J., Sparks, W.B., van Spanning, R.J.M., Röling, W.F.M., and Snik, F. (2017) Circular spectropolarimetric sensing of chiral photo-systems in decaying leaves. *J Quant Spectrosc Radiat Transf* 189:303–311.
- Pertenais, M., Neiner, C., Bouillot, A., Vachey, M., Folsom, C.P., and Gómez de Castro, A.I. (2017) Optical design of Arago's spectropolarimeter. *Proc SPIE* 10562, doi:10.1117/12.2296215.
- Pizzarello, S., and Cronin, J.R. (2000) Non-racemic amino acids in the Murray and Murchison meteorites. *Geochim Cosmochim Acta* 64:329–338.
- Pizzarello, S., Schrader D., Monroea A., and Lauretta D. (2012) Large enantiomeric excesses in primitive meteorites and the diverse effects of water in cosmochemical evolution. *Proc Natl Acad Sci USA* 109:11949–11954.
- Rosenbush, V., Kolokolova, L., Lazarian, A., Shakhovskoy, M., and Kiselev, N. (2007) Circular polarization in comets: observations of comet C/1999 S4 (LINEAR) and tentative interpretation. *Icarus* 186:317–330.
- Rotundi, A., Sierks, H., Della Corte, V., Fulle, M., Gutierrez, P.J., Lara, L., Barbieri, C., Lamy, P.L., Rodrigo, R., Koschny, D., et al. (2015) Dust measurements in the coma of comet 67P/Churyumov-Gerasimenko inbound to the Sun. *Science* 347, doi:10.1126/science.aaa3905.
- Sandford, S.A., Nuevo, M., Bera, P.P., and Lee, T.J. (2020) Prebiotic astrochemistry and the formation of molecules of astrobiological interest in interstellar clouds and protostellar disks. *Chem Rev* 120:4616–4659.
- Silverman, M.P., and Badoz, J. (1990) Light reflection from a naturally optically active birefringent medium. *J Opt Soc Am A Opt Image Sci Vis* 7:1163–1173.
- Sparks, W.B., Hough, J., Germer, T.A., et al. (2009a) Detection of circular polarization in light scattered from photosynthetic microbes. *Proc. Natl Acad Sci USA* 106:7816–7821.
- Sparks, W.B., Hough, J., Kolokolova, L., et al. (2009b) Circular polarization in scattered light as a possible biomarker. *J Quant Spectrosc Radiat Transfer* 110:1771–1779.
- Tanaka, M., Kaneko, F., Koketsu, T., Nakagawa, K., and Yamada, T. (2008) Fragmentation and dimerization of aliphatic amino acid films induced by vacuum ultraviolet irradiation. *Radiation Physics and Chemistry* 77:1164–1168.
- Tranter, G.E., and McDermott A.J. (1989) Electroweak bio-nantioselection. *Chem Phys Lett* 163:1–4.
- Tozzi, G.P., Feldman, P.D., and Festou, M.C. (1998) Origin and production of C(¹D) atoms in cometary comae. *Astron Astrophys* 330:753–763.
- Weaver, H.A., Feldman, P.D., Festou, M.C., A'Hearn, M.F., and Keller, H.U. (1981) IUE observations of faint comets. *Icarus* 47:449–463.
- Wickramasinghe, N.C. (1974) Formaldehyde polymers in interstellar space. *Nature*, 252:462–463.

Address correspondence to:
 Prof. Ana I. Gómez de Castro
 Fac. CC Matemáticas
 Universidad Complutense de Madrid
 Plaza de Ciencias 3
 28040 Madrid
 Spain

E-mail: aig@ucm.es

Submitted 2 June 2020

Accepted 1 February 2021

Associate Editor: Christopher McKay

Abbreviations Used

CD = circular dichroism
 COS = Cosmic Origins Spectrograph
 CPR = circularly polarized radiation
 ee = enantiomeric excess
 HST = Hubble Space Telescope
 IUE = International Ultraviolet Explorer
 L = left-handed
 ORD = optical rotatory dispersion
 R = right-handed
 SNR = signal-to-noise ratio
 STIS = Space Telescope Imaging Spectrograph
 UV = ultraviolet